CHAPTER 1 — WIND

CHAPTER 1 — WIND

1.1 Winds in the free atmosphere

1.1.1 Geostrophic wind (V_g)

V_g is defined as the steady (unaccelerating), horizontal wind which results from the balance of two forces only — namely the pressure gradient force and the Coriolis force, f. It follows that geostrophic wind is a good approximation to the actual wind only with isobars (or contours) which are straight, parallel and not changing with time. There are significant differences from V_g in strongly curved flow and flow near surfaces.

On MSL charts, or any other chart at a constant height level:

$$V_g = (1/\rho f)\,|\Delta p/\Delta n|$$

where Δn is measured normal to the isobars and V_g blows with low pressure to the left in the northern hemisphere; ρ is the air density. Similarly on charts at a constant pressure level:

$$V_g = (g/f)\,|\Delta z/\Delta n|$$

where $|\Delta p/\Delta n|$ is the scalar horizontal pressure gradient (in hPa m^{-1}), $|\Delta z/\Delta n|$ is the height gradient along a constant pressure surface (in m m^{-1}) and V_g is expressed in m s^{-1}.

(Note: The Rossby Number, V_g/fL (where L is a scale length) is a useful measure of the validity of the geostrophic approximation; the smaller the value the smaller the ageostrophic contribution.)

1.1.1.1 Tables for geostrophic winds

Table 1.1 may be used to derive V_g for charts on which no geostrophic wind scale is provided. It gives 'multipliers' corresponding to a pressure (contour height) change over a distance of 300 n mile (or 5° latitude) of 1 hPa (1 dam).

Examples:

(i) A gradient of 5 hPa per 300 n mile at 55° N corresponds to $V_g = 5 \times 2.4 = 12$ kn (approx.).

(ii) A gradient of 12 dam per 300 n mile at 50° N corresponds to $V_g = 12 \times 3.1 = 37$ kn (approx.).

Table 1.1. To derive V_g for charts with no geostrophic scale

	Pressure/height change over 300 n mile	
	Isobars (hPa)	Contours (dam)
Latitude (°)	multipliers	
70	2.1	2.5
60	2.3	2.7
55	2.4	2.9
50	2.6	3.1
45	2.8	3.3
40	3.1	3.7
35	3.4	4.1
30	3.9	4.7

If gradients are measured over shorter distances, the factors should be altered in proportion, i.e. for 150 n mile (2.5° latitude span) the factors are doubled. Correction factors for density variations may be applied to geostrophic wind values measured by scales based on the Standard Atmosphere (1013.2 hPa, 15 °C) as follows:

Table 1.2. Percentage corrections to geostrophic wind

Pressure	Temperature (°C)								
(hPa)	+40	+30	+20	+10	0	−10	−20	−30	−40
920	120	116	112	108	104	101	97	93	89
940	117	113	110	106	102	98	95	91	87
960	115	111	107	104	100	96	93	89	85
980	112	109	105	102	98	94	91	87	84
1000	110	107	103	100	96	93	89	85	82
1020	108	104	101	98	94	91	87	84	80
1040	106	102	99	96	92	89	86	82	79
1060	104	101	97	94	91	87	84	81	77

Example:
If the measured $V_g = 25$ kn at a location where the pressure is 1030 hPa and the temperature is −10 °C, then the true $V_g = 25 \times 90\% = 22.5$ kn.

1.1.2 Gradient wind

When its trajectory is curved, air must be subjected to a local centripetal acceleration, V^2/r, where V is the gradient wind velocity and r is the radius of curvature of the trajectory.

The gradient wind equations are:

(i) for cyclonic curvature:
$V_{gr} = 0.5[- rf + (r^2f^2 + 4rf\,V_g)^{0.5}]$ gradient wind is sub-geostrophic;

(ii) for anticyclonic curvature:
$V_{gr} = 0.5[+ rf - (r^2f^2 - 4rf\,V_g)^{0.5}]$ gradient flow is super-geostrophic.

1.1.2.1 Estimation of gradient wind (tabular method)

Corrections to be applied to the geostrophic wind to obtain the gradient wind are given in **Table 1.3**. The top section of the table (a) shows how changes in the Coriolis parameter affect the results. Thus a radius of **600** n mile at latitude 50° is equivalent to a radius of **489** n mile at latitude 70° or **919** n mile at latitude 30°.

1.1.2.2 Estimation of gradient wind (graphical method)

Fig. 1.1 is a graph for obtaining the gradient wind speed from the speed of the geostrophic wind and the radius of curvature. The graph is drawn for use at latitude 50°. For use at other latitudes the radius of curvature must be multiplied by a correction factor to obtain the equivalent value at latitude 50°.

To use the graph:

(i) Use the right-hand inset to find the equivalent radius of curvature for latitudes other than 50°. Multiply the actual radius by the factor shown against the value for latitude. If, for example, the radius at latitude 39.5° N is 1200 n mile, the correction factor is 0.83 and the equivalent radius at latitude 50° is about 1000 n mile.

(ii) Find the point of intersection of the geostrophic wind speed (shown along the left-hand axis) with the curve showing the radius of curvature. The cyclonic curves lie to the left and the anticyclonic curves lie to the right of the straight line denoting infinite radius. The gradient wind speed is shown along the bottom of the diagram. Thus with a radius of curvature of 1000 n mile and $V_g = 90$ kn, the gradient wind is 76 kn for cyclonic curvature and 136 kn for anticyclonic curvature.

The theoretical maximum gradient wind speed for anticyclonic curvature is twice the geostrophic wind. The graphs show that as the gradient wind approaches this value, small increases in the geostrophic wind can produce very large increases in the gradient wind.

Table 1.3. Gradient wind corrections

(a)

Latitude (°)	Radius of curvature of isobar or contour (n mile)											
70	98	147	196	245	367	**489**	737	978	1467	1957	2446	3261
60	106	159	212	265	398	531	796	1061	1592	2123	2654	3538
50	120	180	240	300	450	**600**	900	1200	1800	2400	3000	4000
40	143	215	286	358	536	715	1073	1430	2145	2860	3575	4767
30	184	276	368	460	689	**919**	1379	1839	2758	3677	4596	6128

The corrections are to be applied to the geostrophic wind to obtain the gradient wind when the system of isobars or contours is stationary.

(b)

Geostrophic speed (kn)	Cyclonic curvature correction (kn)											
10	−1	−1	−1	−1	0	0	0	0	0	0	0	0
20	−5	−4	−3	−3	−2	−1	−1	−1	−1	0	0	0
30	−9	−7	−6	−5	−4	−3	−2	−2	−1	−1	−1	−1
40	−14	−11	−10	−8	−6	−5	−4	−3	−2	−2	−1	−1
60	−25	−21	−18	−16	−12	−10	−8	−6	−4	−3	−3	−2
80	−37	−32	−28	−25	−20	−17	−13	−10	−7	−6	−5	−4
100	−51	−44	−39	−35	−28	−24	−18	−15	−11	−9	−7	−6
120	−64	−56	−50	−46	−38	−32	−25	−21	−15	−12	−10	−8
140	−78	−69	−62	−57	−47	−41	−32	−27	−20	−16	−13	−10
160	−93	−83	−75	−69	−58	−50	−40	−33	−25	−20	−17	−13
180	−108	−96	−88	−81	−69	−60	−48	−40	−31	−25	−21	−16
200	−123	−111	−101	−94	−80	−70	−57	−48	−37	−30	−25	−20

(c)

Geostrophic speed (kn)	Anticyclonic curvature correction (to be added) (kn)											
10	4	2	1	1	1	0	0	0	0	0	0	0
20	—	—	8	5	3	2	1	1	1	0	0	0
30	—	—	—	26	8	5	3	2	1	1	1	1
40	—	—	—	—	20	11	6	4	2	2	1	1
60	—	—	—	—	—	52	16	10	6	4	3	2
80	—	—	—	—	—	—	39	21	12	8	6	4
100	—	—	—	—	—	—	—	41	20	13	10	7
120	—	—	—	—	—	—	—	104	32	20	15	11
140	—	—	—	—	—	—	—	—	50	30	22	15
160	—	—	—	—	—	—	—	—	79	42	30	20
180	—	—	—	—	—	—	—	—	156	59	40	26
200	—	—	—	—	—	—	—	—	—	83	53	34

1.1.2.3 Curvature of trajectories for systems in motion

Significant differences occur between the curvature of trajectories and the curvature of isobars or contours when the systems are in motion (**Fig. 1.2**).

In (a) the eastward moving depression has a speed of half the geostrophic wind around it, while (b) has a speed twice the geostrophic. Calculated parcel trajectories take into account the locally changing pressure pattern. Trajectory curvature is much less than isobaric curvature on southern and western sides, greater on northern and eastern sides. Thus winds could be super-geostrophic on the south-western side (assuming even isobaric spacing) of a fast-moving depression, and certainly stronger than those in the north-eastern sector.

Holton (1992)

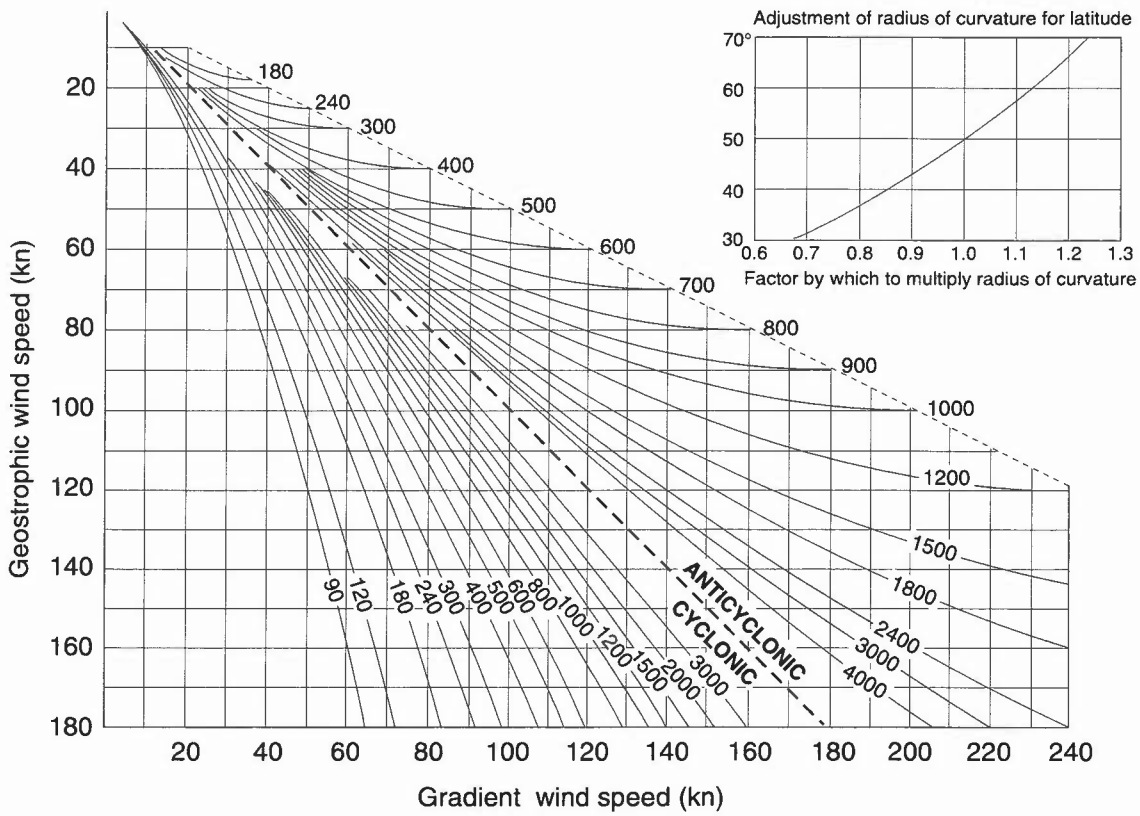

Figure 1.1. A graph to obtain the gradient wind speed from the speed of the geostrophic wind and the radius of curvature.

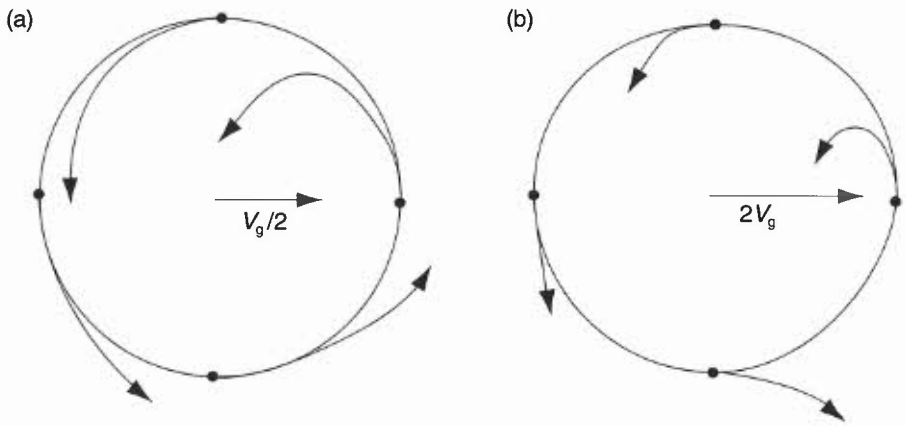

Figure 1.2. (a) Calculated trajectories of parcels of air around a depression moving eastwards at half the geostrophic wind speed. (b) Calculated trajectories of parcels of air around a depression moving eastwards at twice the geostrophic wind speed.

1.1.3 Variations in the mean wind

1.1.3.1 Ageostrophic winds (see Chapter 8)

An actual wind may be considered to have two components, one of which is geostrophic and the other ageostrophic (non-geostrophic).

1.1.3.2 Thermal winds

(i) The *thermal wind* in the layer between two pressure levels is the vector difference between the geostrophic winds at two levels B (upper level) and A (lower level) (**Fig. 1.3**).
Thus: $V_{\text{thermal}} = V_A - V_B$.

(ii) A geostrophic wind is proportional to the contour height gradient at a pressure level; a thermal wind, $V_{thermal}$, measures the difference in the contour gradient between two pressure levels. $V_{thermal}$ is proportional to the horizontal temperature gradient in the layer. It may be regarded as a steering wind for surface features.

(iii) A strong north–south temperature gradient implies a strong westerly thermal wind with a westerly wind component increasing with height in the layer. A reversed temperature pattern gives easterly thermal winds, and a westerly wind component decreasing with height.

(iv) Although the thermal wind is geostrophic, practical computations use the difference between the actual winds at two levels. This is normally acceptably accurate.

Holton (1992)

1.1.4 Use of the hodograph

Plotting

Wind vectors are plotted on a hodograph so that they end at the centre of the diagram. **Fig. 1.3** shows a 900 hPa wind of 240° 20 kn and an 800 hPa wind of 300° 30 kn. The thermal wind in this layer is the vector from B to A. A normal hodograph plot only shows the points at each pressure level, joined to show the thermal winds in each layer.

Identifying the direction of warm and cold air

In **Fig. 1.4** the colder air is shown by light stippling and the warmer air by heavy stippling. Arrows show the direction of the thermal winds in the different layers. Thus between 850 and 500 hPa the thermal wind direction is 240° which shows that the colder air lies towards the north-west. Between 500 and 400 hPa the thermal wind direction is 005° indicating that in that layer the colder air is towards the east.

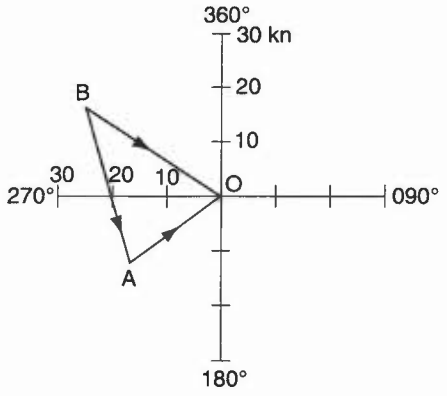

Figure 1.3. Plotting wind vectors on a hodograph. AO is the lower-level wind vector (say, 900 hPa). BO is the upper-level wind vector (say, 800 hPa). BA is the thermal wind vector (directed from the upper to the lower wind vectors).

Warm and cold advection

Between 900 and 850 hPa in **Fig. 1.4** the thermal wind direction is 315°, indicating colder air to the north-east. Since the mean wind direction between these levels is from the north-east, colder air is being advected towards the station. This cold advection is in fact taking place at all levels up to 500 hPa. (i.e. wind is backing with height). Between 500 and 400 hPa the thermal wind is from 005° while the mean wind is about 345° indicating weak warm advection (wind is veering with height).

1.1.4.1 Fronts and vertical motion

Fig. 1.5 shows a construction which can be useful when a frontal surface lies over the station at some level.

(i) Mark the surface front through the centre of the hodograph, its orientation being as shown on a surface chart.

(ii) Determine the upper and lower levels of the frontal zone from a tephigram (i.e. noting change of θ_w), and mark them on the hodograph. The thermal wind direction in the frontal zone is often roughly parallel to the front.

(iii) Measure the wind component normal to the front at each level in the frontal zone and in the warm air mass above.

(iv) The frontal speed at the surface approximates to the speed of the cold air normal to the front at the base of the frontal zone (although adiabatic effects often lead to this being an overestimate).

(v) If the wind component normal to the front increases with height in the warm air, then: a warm front is an anafront, and a cold front is a katafront.

(vi) If the wind component normal to the front decreases with height in the warm air, then: a warm front is a katafront, and a cold front is an anafront.

HWF (1975), Chapter 3.4.3

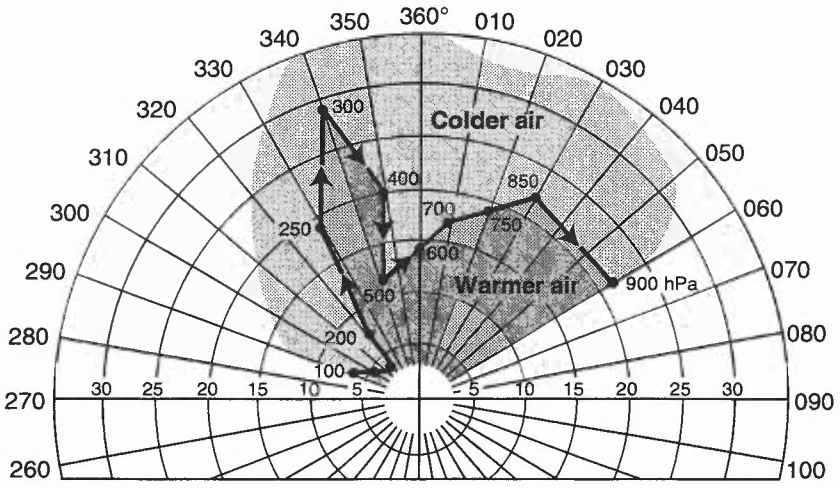

hPa	deg	kn
900	060	22
850	030	22
750	020	19
700	010	17

hPa	deg	kn
600	360	14
500	340	12
400	350	20
300	340	29

hPa	deg	kn
250	330	18
200	320	7
150	320	4
100	300	6

Figure 1.4. Hodograph example: Stornoway, 0600 UTC on 9 June 1961.

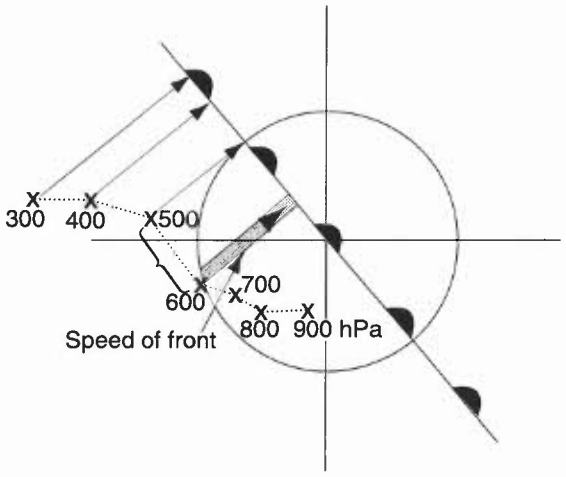

Figure 1.5. Assessment of ana- and kata-frontal characteristics from a hodograph.

1.1.5 Jet streams

1.1.5.1 The polar-front jet

(i) This is so named for its links with the polar front.
(ii) This jet is found over a wide range of latitudes between 35° and 70°.
(iii) The mean position is nearer the equator in winter than in summer.

A cross-section through a typical example of a polar-front jet is shown in **Fig. 1.6**, and the relationship between the location of surface fronts and jet core in a mature system in **Fig. 1.7**.

Height

(i) The jet core is located in the warm air about 3000 ft below the tropopause, usually between 300 and 250 hPa, and vertically above the position of the frontal zone at 500 hPa.
(ii) The level varies along the length of the jet, being higher round ridges and lower near troughs.

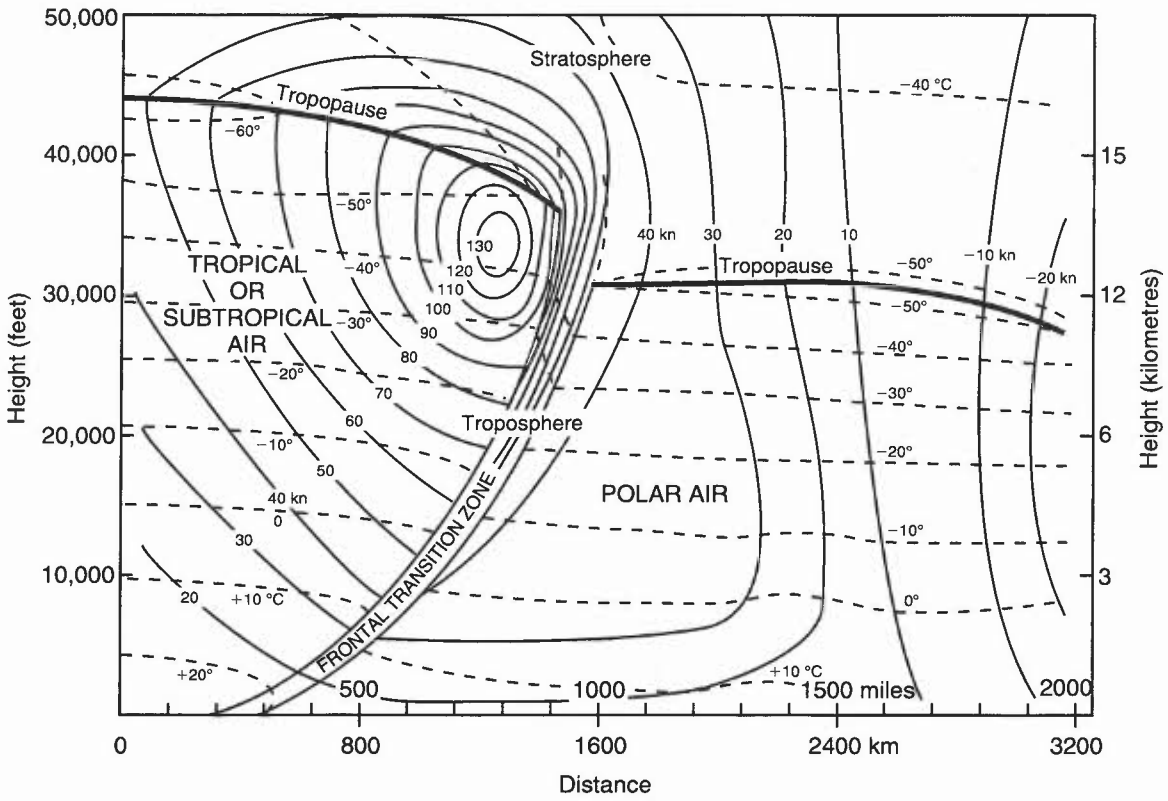

Figure 1.6. Cross-section across a polar-front jet stream. Solid lines are isotachs (knots) and broken lines isotherms (°C). Positive wind speeds have a component out of the plane of the page.

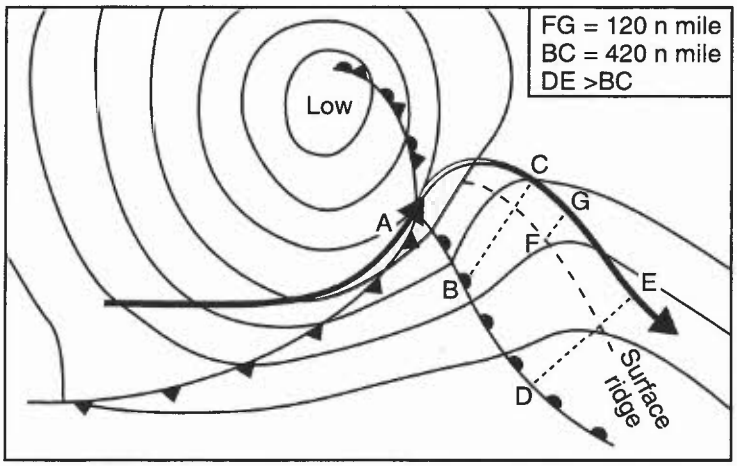

Figure 1.7. Polar-front jet in relation to surface fronts. The broad arrow represents the core of the jet at 300 hPa, which is weak or broken in the unshaded section. A is the tip of the warm sector.

Direction:

(i) The majority of jets have a component from between 190° and 350°.

(ii) Northerly or north-easterly jets occur at times in the winter months. South-easterly jets are rare.

Speeds

(i) Winter jets can often reach 150 kn and may sometimes exceed 200 kn.

(ii) The 300 hPa wind speed is approximately twice the maximum thermal wind in the 500 to 1000 hPa layer, but displaced some 60 n mile to the cold side of the thermal wind maximum.

(iii) The core of a jet at any level crosses the contour pattern on the entrance and exit regions of a jet, due to ageostrophic effects **(Fig. 1.8)**. (See 8.2).

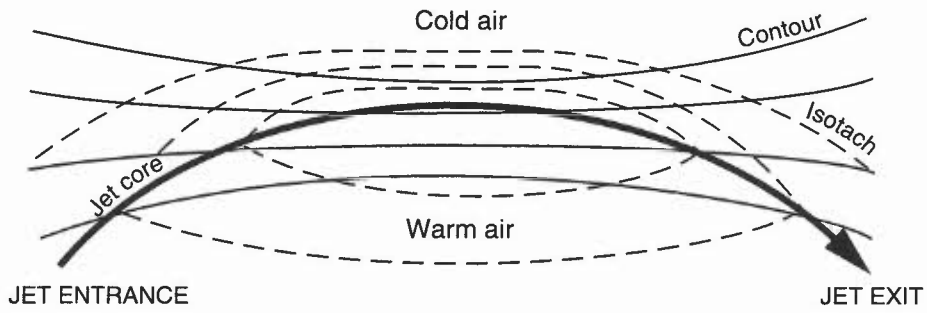

Figure 1.8. Position of the jet core on an upper-level chart, in relation to the contour lines. In the entrance and exit regions, ageostrophic effects produce cross-contour flows. In the steady part of the jet the core is displaced towards the cold side of the contour pattern.

Vertical shear

This varies in relation to the strength of the jet **(Table 1.4)**:

Table 1.4. Vertical shear associated with jet streams

Typical values:	
Normal	3–6 kn per 1000 ft
Large	10–15 kn per 1000 ft
Extreme	more than 20 kn per 1000 ft

(i) The maximum horizontal shear is generally on the cold side of the jet at about the core level, or slightly below.
(ii) On the warm side of the jet the maximum anticyclonic shear is slightly above the core level.
(iii) Theoretically the anticyclonic shear cannot exceed the Coriolis parameter which has values as follows **(Table 1.5)**.

Table 1.5. Coriolis parameters

Latitude (°)	30	35	40	45	50	55	60	65	70
Coriolis parameter (kn/100 n mile)	26	30	34	37	40	43	45	47	49

When the warm-side maximum shear values are attained, or exceeded, the flow becomes turbulent.

1.1.5.2 The subtropical jet

The subtropical jet generally occurs between latitudes 20 and 30° and is most marked during the winter months.

1.1.5 3 Overlapping of jets

(i) Satellite pictures show that a cyclonically curved polar-front jet may cross underneath the anticyclonically curved subtropical jet.
(ii) There are then two velocity maxima, one near 200 hPa and the other near 300 hPa.
(iii) Very sharp changes of wind direction can occur in the relatively shallow layer between the two jet cores, resulting in severe clear air turbulence (CAT).

HAM (1994)

1.2 Winds near the surface

Forecasts required will depend on what is at risk and the nature of the wind/gust hazard.

Hunt (1995)

1.2.1 *Surface wind and gradient wind*

(i) The surface wind is usually reduced in speed and backed in direction from the gradient wind (**Fig. 1.9**).

(ii) The magnitude of the change depends on the stability of the air and the roughness of the surface. Rough surfaces increase the frictional effect; greater stability reduces the turbulent exchange of energy between the flow aloft and that at the surface. An increase in stability near the surface implies a change in the vertical wind profile.

1.2.1.1 *Surface wind and 900 m wind (statistical relations)*

Table 1.6 shows some observed relationships between the speed of the surface wind (V_0) and the 900 m wind (V_9), together with the angle (α) between them.

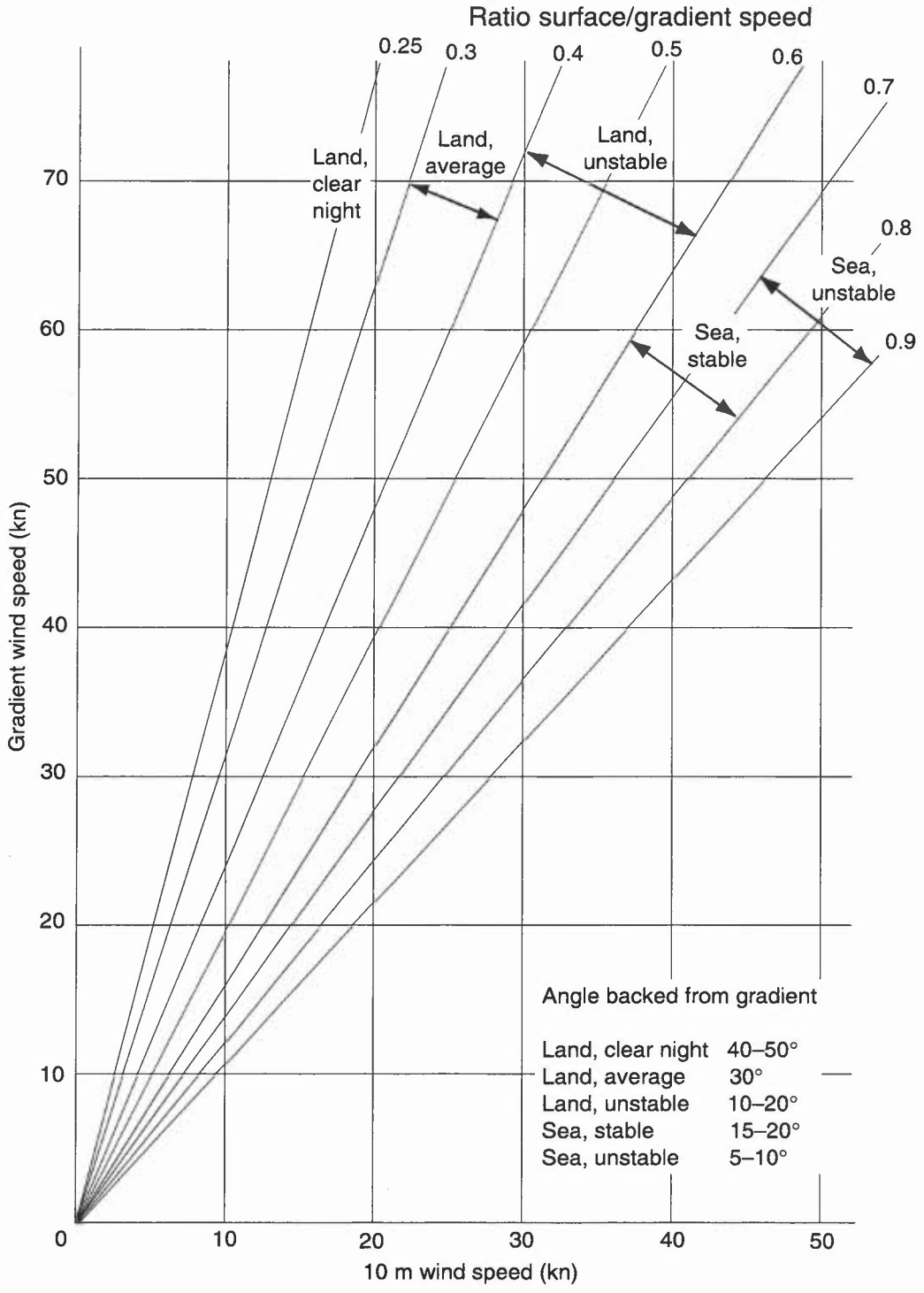

Figure 1.9. Nomogram for determining the 10 m wind speed and direction from gradient wind speed in various conditions of stability and surface roughness (the numbers on the diagonal lines represent the ratio of surface/gradient speed).

Lapse-rates are classified as:

1. Superadiabatic.
2. Conditionally unstable.
3. Conditionally stable.
4. Stable.
5. Isothermal/Inversion*.

*Important from the aviation point of view is the breaking up of the surface inversion with the consequent increase in mean surface wind

(The above lapse rate classes are based on the difference between surface and 900 hPa temperatures, differences which may not reflect the boundary-layer stability all that well.)

Table 1.6. Observed relationships between the speed of the surface wind (V_0) and the 900 m wind (V_9) together with the angle (α) between them

(a) Over the sea: at 59° N, 19° W and 52° N, 20° W

Lapse class	900 m wind speed (kn) 10–19		20–29		30–39		40–49		>50	
	V_0/V_9	α	V_0/V_9	α	V_0/V_9	α	V_0/V_9	α	V_0/V_9	α
1	0.95	0	0.90	0	0.85	0	0.80	0	0.80	0
2	0.90	5	0.85	5	0.80	5	0.75	5	0.75	5
3	0.85	10	0.75	10	0.70	10	0.65	10	0.65	10
4	0.80	15	0.70	20	0.65	20	0.60	20	0.60	20
5	0.75	15	0.70	20	0.65	20	0.60	20	0.55	25

(b) Over land: at London (Heathrow) Airport

Lapse class	900 m wind speed (kn) 10–19		20–29		30–39		40–49		>50	
	V_0/V_9	α	V_0/V_9	α	V_0/V_9	α	V_0/V_9	α	V_0/V_9	α
Daytime										
1, 2	0.65	5	0.55	5	0.50	10	0.50	10	0.35	15
3	0.50	20	0.45	20	0.45	20	0.45	20	0.45	15
4	0.45	35	0.45	30	0.40	25	0.30	20	0.40	25
5	0.35	45	0.40	35	0.35	35	0.40	30	0.40	30
Night-time										
1, 2	0.25	20	0.35	25	0.30	35	0.40	15	0.40	25
3	0.35	25	0.35	30	0.35	25	0.35	20	0.35	15
4	0.30	35	0.30	35	0.30	30	0.35	30	0.35	15
5	0.30	45	0.25	40	0.25	35	0.30	30	No obs	

(Some results based on less than 10 observations.)

Fig. 1.9 is a useful first-guide summary based on these figures.

Two sets of these analyses, using sectored wind directions with wind-speed bands to include the 2–10 kn range, and based on 3-monthly data sets from two appropriate radiosonde stations (for 00/12 UTC), enables a realistic estimate to be made (to be checked against model output) of the mean surface wind speed for local normal aircraft operations and TAFs.

Findlater et al. (1966)

1.2.2 Vertical wind shear

1.2.2.1 Vertical wind shear over surfaces with different roughness

(i) For neutral stability (defined as a dry adiabatic lapse rate throughout) the variation of wind speed (V) with height (z) may be expressed by: $V(z)/V(10) = \ln(z/z_o)/\ln(10/z_o)$ where z_o depends on the roughness of the terrain.

(ii) This relationship is considered reasonable to 100 m or so and is probably usable above that.

(iii) **Fig. 1.10** shows the calculated ratio V_z/V_{10} (the winds at z and 10 metres) for different surfaces.

(iv) The curves show that over wooded country:
if the 200 m wind is 18 kn, then the 100 m wind should be just under 16 kn and the 10 m wind should be 10 kn.

Table 1.7 gives the variation with height of the mean hourly wind and corresponding gusts, based on statistical data, and likely to be particularly applicable to open areas under neutral conditions.

Local Weather Manuals (1994)

Table 1.7(a). Variation with height of mean hourly wind speeds (knots) in open level situations calculated according to the formula $V_H = V_{33}((H^{0.17})/33)$

Standard effective height			Effective heights (H)			
33 ft	70 ft	100 ft	150 ft	200 ft	250 ft	300 ft
10	11	12	13	13	14	15
15	17	18	19	20	21	22
20	23	24	26	27	28	29
25	28	30	32	34	35	36
30	34	36	39	41	42	44
35	40	42	45	47	49	51
40	45	48	52	54	56	58
45	51	54	58	61	63	65
50	56	60	65	68	70	73
55	62	66	71	75	77	80
60	68	72	78	82	85	87

Table 1.7(b). Variation with height of gusts speeds (knots) in open level situations calculated according to the formula $V_H = V_{33}((H^{0.085})/33)$

Standard effective height			Effective heights (H)			
33 ft	70 ft	100 ft	150 ft	200 ft	250 ft	300 ft
30	32	33	34	35	36	36
35	37	38	40	41	42	43
45	47	49	51	52	53	54
50	53	55	57	58	59	60
55	58	60	62	64	65	66
60	64	66	68	70	71	72
65	69	71	74	76	77	78
70	74	77	80	82	83	84
75	80	82	85	87	89	90
80	85	88	91	93	95	96
85	90	93	97	99	101	102
90	95	99	102	105	107	109
95	101	104	108	111	113	115
100	106	110	114	117	119	121
105	111	115	119	122	125	127
110	117	121	125	128	131	133

Note: The above table represents a useful general guide, but may be misleading in very stable or very unstable conditions, in heavily built-up areas, very hilly ground, etc.

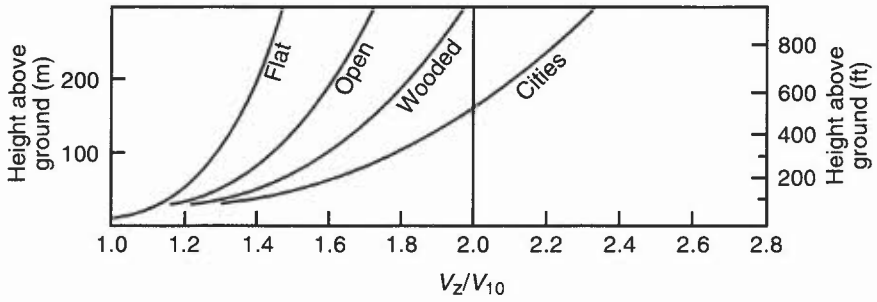

Figure 1.10. Calculated ratio of V_z/V_{10} over different surfaces in neutral stability conditions.

1.2.2.2 Vertical wind shear in different stability conditions

(i) Strong wind shears can be due to high stability, especially with increasing gradient winds.
(ii) There will be orographic/shelter influences.

Fig. 1.11 shows how the ratio V_z/V_{10} alters with changes of stability based on observations of wind changes between the surface and 400 ft with lapse rates ranging from +2 °C to −6 °C through that layer (lapse rate of −6 °C means a rise of 6 °C within the layer).

HWF (1975), Chapter 16.5.2
WMO (1969)

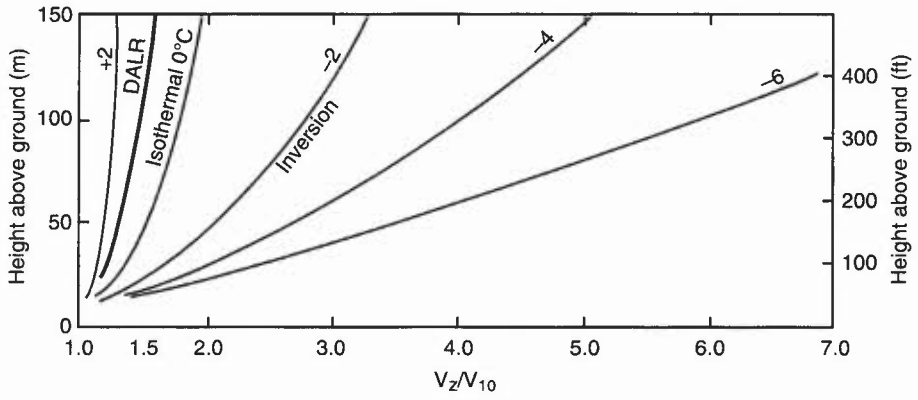

Figure 1.11. Observed ratio of V_z/V_{10} for different lapse-rates, measured at Cardington.

1.2.2.3 Criteria for airfield warnings of hazardous low-level wind shear/turbulence (see 6.2.1.1)

MO, Heathrow (198?)

1.2.2.4 The nocturnal jet and diurnal variations of vertical wind shear

Nocturnal jets can be an embarrassment to light aircraft when landing and will influence pollution transport (and bird migration).

(i) A nocturnal jet can occur overland when radiation cooling over a sufficient period of time (particularly during spring and autumn) stabilizes the near-surface flow (θ increases with height). The frictional force is greatly reduced in the upper part of the boundary layer where speeds become super-geostrophic and undergo an inertial oscillation about the geostrophic value.
(ii) Near the top of the stable layer the wind speed may be 1.5 and sometimes up to 3 times the geostrophic value **(Fig. 1.12).** The inertial period is about 17 hours in mid-latitudes; the magnitude of the geostrophic departure depends on the geostrophic wind departure at the end of the previous day. The jet will not be pronounced in light winds; the inversion cannot form if the wind is too strong.
(iii) The length of the night relative to the half inertial period determines whether the maximum super-geostrophic wind will occur by dawn when the jet becomes important in the subsequent boundary-layer evolution.

(iv) Wind in the lower layer has a cross-isobar angle of 60–70°. Over England speeds of 40 kn have been measured at heights usually below the top of the inversion (≈600 ft) by the end of a radiation night.
(v) By dawn the jet is more pronounced along a direction parallel to the surface geostrophic wind. The speed decreases rapidly after sunrise with jet break-down due mainly to convective activity from surface insolation reaching the jet level 2 to 3 hours after sunrise.
(vi) A helpful indicator of jet formation over rough terrain is if the 10 m wind decreases significantly after dark.

Above conditions are likely to be satisfied in an anticyclonic region of significant pressure gradient; warm advection forcing the development of mesoscale convective systems (4.7) is often associated with the nocturnal jet.

As an example of vertical wind shear: associated with a nocturnal 'jet', observed at Cardington on a radiation night, was a wind-speed shear of 0.42 kn m^{-1} (15 kn between 9 m (30 feet) and 45 m (150 feet)).

Downward momentum transfer is an important consideration for night aviation forecasts; it can maintain light surface winds over airfields on ridges and small hills, keeping them from visibility deterioration that might occur in the valley. Conversely, diurnal reversal after sunrise may result in deteriorating conditions of fog/low stratus.

Stull (1988)
Thorpe & Guymer (1977)

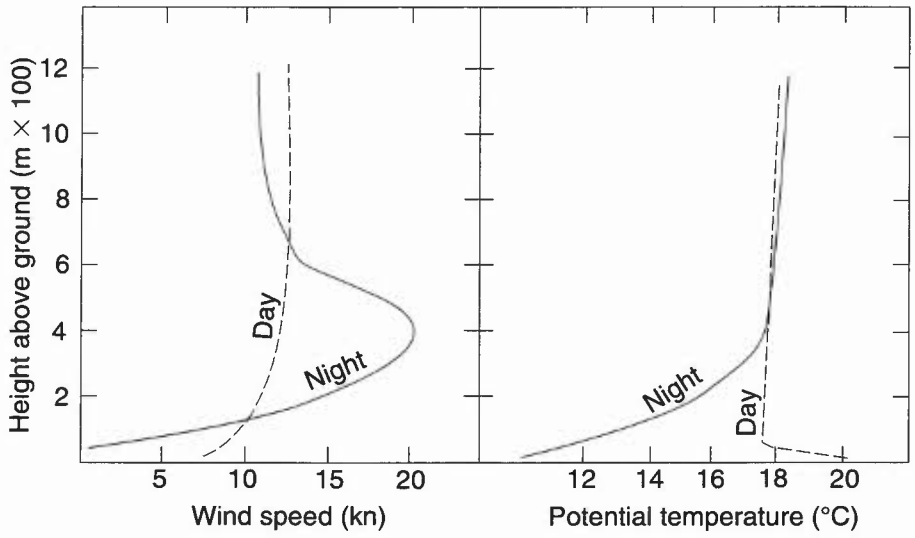

Figure 1.12. Vertical profiles of wind speed and potential temperatures by night and day under typical fair-weather conditions with little or no low cloud.

1.2.3 Low-level jets

(i) These are bands of strong winds in the lower troposphere.
(ii) Unlike high-level jets there is no specified minimum speed and many do not exceed 60 kn.
(iii) These jets are often associated with large vertical and horizontal wind shears.
(iv) Low-level jets occur in the warm conveyor belt just ahead of a surface cold front.
(v) There may be more than one core, each about 100 km wide.
(vi) Maximum speeds are in the range 50–60 kn and at a height of about 1 km.

A cross-section through one example of a low-level jet associated with a front is at **Fig. 1.13**.

1.3 Local winds

1.3.1 Sea and land breezes

Sea (and land) breezes are driven by the unequal diurnal heating and cooling of adjacent land and sea surfaces.

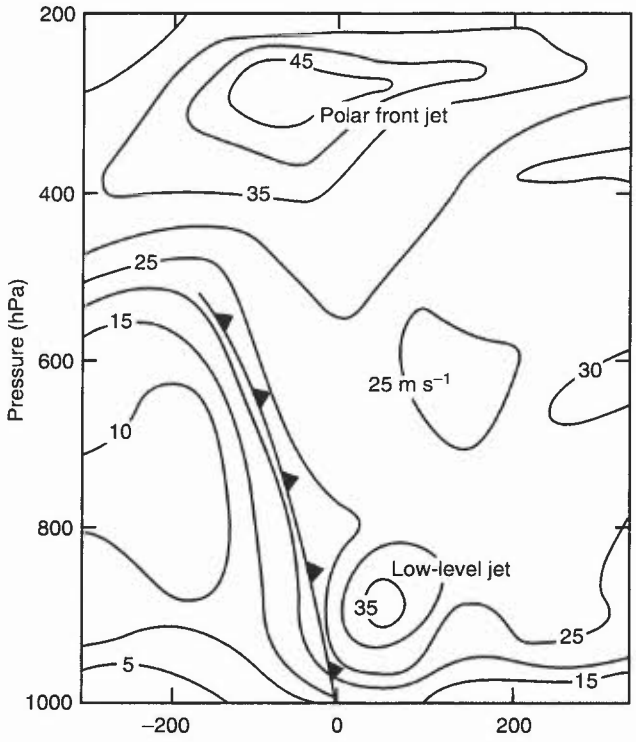

Figure 1.13. Low-level 'jet' associated with a front. Isotachs at intervals of 5 m s^{-1} show the wind flow into the paper.

1.3.1.1 Sea breezes

Criteria for sea breezes:

(i) inland temperatures greater than temperature of coastal waters;

(ii) a moderate depth of dry convection to, say, between 750 and 900 m (2500 to 3000 ft) is required before the sea breeze can become established;

(iii) if the air is so stable that the convection is confined to a very shallow layer there will be little or no penetration of the sea-breeze regardless of the temperature difference between land and sea;

(iv) only a weak offshore wind component of <14 kn at 3000 ft initially;

(v) convection to 1500 m (4000 ft) favours deep inland penetration (deep convection, leading to shower or thundery activity, tends to halt the sea-breeze);

(vi) significant inland penetration is only likely if offshore 3000 ft wind is <10 kn. This is typified by the following observations **(Table 1.8)** for the onset of sea breezes as a function of land/sea temperature contrast for the Lincolnshire coast.

Table 1.8.

Off-shore component (kn)	2	4	6	8	10	12	14	16
Temperature contrast (°C)	3.5	5.0	6.0	7.3	9.0	11	14	—

(sea surface temperature measured at light vessel in 19 m of water, 30 miles (48 km) offshore).

Providing these criteria are met the approximate time for a sea breeze to start to move inland is given by **Table 1.9:**

Table 1.9.

Off-shore wind component (kn) at 3000 ft	Time sea-breeze front crosses coast (UTC)
≥15	sea-breeze front unlikely
14	1600
10	1100–1200
5	0900 (or when convection penetrates 3000 ft)

Sea-breeze front

(i) The convergence line where incoming sea air meets the land air is often termed the sea-breeze front.

(ii) A small off-shore component to the geostrophic wind is generally needed for the development of a well defined front.

(iii) A narrow line of rising air occurs along the front producing enhanced convection; a distinguishing feature is a ragged line of 'curtain cloud hanging below the main cloud base'. Nearly all cloud disperses on the seaward side of the front.

Penetration inland

(i) Movement inland from the coast may extend to more than 50 n mile inland over the south and east of England (10.3.1.1).

(ii) The distance depends on the off-shore component of the geostrophic wind, the land–sea temperature contrast, the depth of convection and the topography.

(iii) High ground delays or deflects the flow of sea air which tends to move up wide valleys rather than climb over hills (**Fig. 1.14**).

(iv) The sea breeze will veer with time.

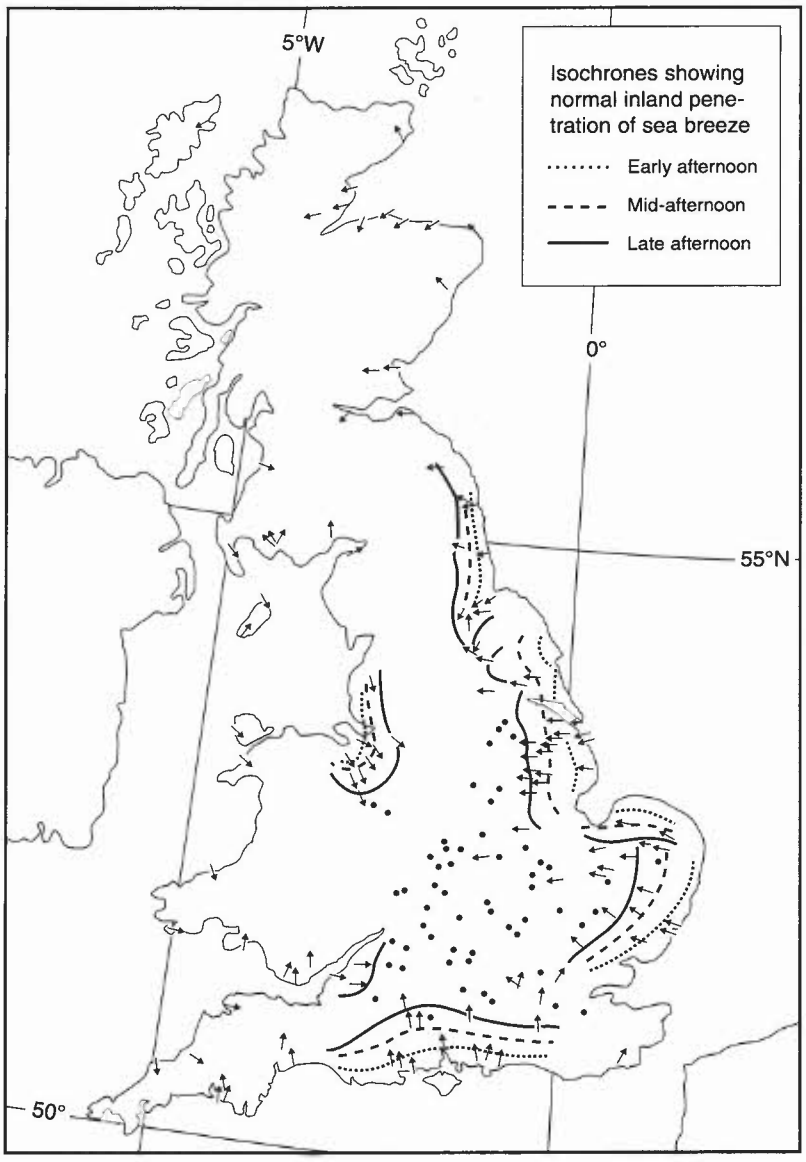

Figure 1.14. The normal direction and penetration of sea-breezes during summer months. Each arrow or dot represents an individual airfield. Arrows show the late afternoon direction of the sea-breeze (a few places having two preferred directions). Dots show airfields where sea-breezes have not been specially recorded in the local weather notes. The isochrones show the normal rate of progress inland of the sea-breeze on a summer afternoon.

Speed of movement

(i) The average in the United Kingdom is 4–8 km h^{-1} (2.2–4.4 kn).

(ii) The rate of advance is not constant. The front moves inland in a series of surges with a speed less than that of the incoming sea air.

Seasonal variation

(i) In the United Kingdom sea-breezes occur from March to late September.

(ii) The majority occur from May to August with the peak in June.

Depth of sea air

(i) The incoming sea air often extends to a height of 2000 ft (600 m), occasionally 3000 ft (900 m), at the front where the depth is greatest.

(ii) The top descends to about half the maximum after the front has passed; visibility may be reduced due to increased relative humidity of air and hygroscopic nature of salt aerosol or to smoke/haze trapped beneath the inversion (e.g. in south-east England) (3.9).

Coastal convergence/divergence effects

Fig. 1.15 shows typical cloud patterns generated by land and sea breezes along peninsulas and inlets; coastal convergence/divergence zones with associated cloudiness are illustrated in **Fig. 1.16.**

Bader et al. (1995), Chapter 6
Bradbury (1989)
Brittain (1970)
Findlater (1964)
HWF (1975), Chapter 16
MG (1991)
Pielke (1984)
Simpson (1994)

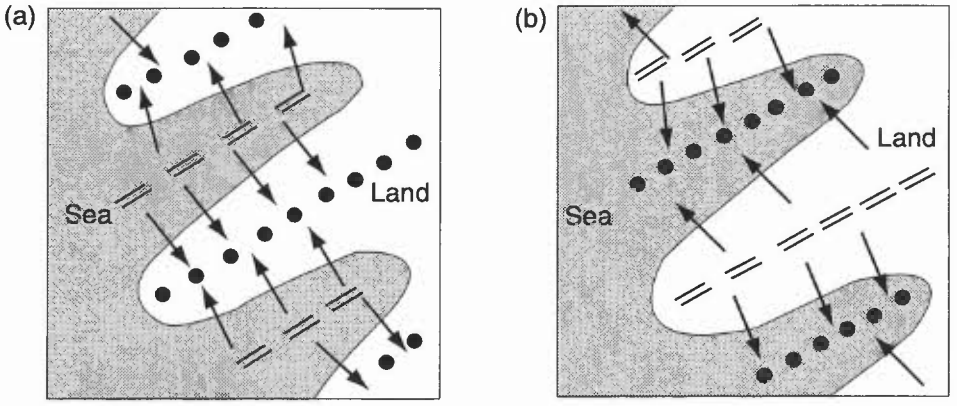

Figure 1.15. Peninsular and inlet convection patterns generated by coastal breezes, showing cloudy areas of surface convergence (····) and cloud-free area of surface divergence (====). (a) On a warm summer day, and (b) when land is relatively cold.

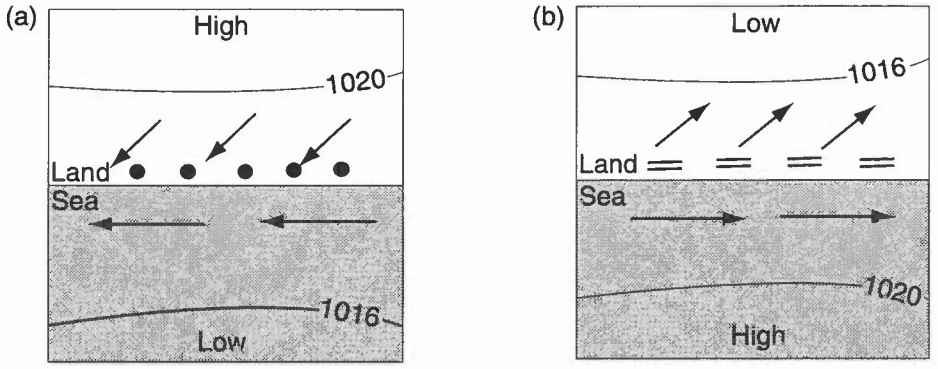

Figure 1.16. Coastal convergence/divergence zones, with cloudiness indicated as in Fig. 1.15. Nominal isobars in hectopascals; arrows are surface wind vectors.

1.3.1.2 The (nocturnal) land breeze

Occurrence

(i) usually sets in about midnight or later;
(ii) it is usually shallower and less well-developed than the sea breeze;
(iii) it is much influenced by topography and tends to increase during the night near flat coasts; a katabatic flow from hills parallel to the coast may reinforce it;
(iv) the strength and frequency depend, theoretically, on the land-sea temperature contrast, and thus might be expected to be greater in anticyclonic conditions in early autumn;
(v) snow-covered ground encourages persistent flow.

Moffitt (1956)

1.3.2 Airflow over hills

1.3.2.1 Mountain waves

Moving, statically stable air, within a boundary layer of thickness δ oscillating at its natural (Brunt–Väisälä) frequency, N:

$$N^2 = (g/\theta)d\theta/dz,$$

traces a wave which has a wavelength Λ. When the (undisturbed) air flow, V, encounters a hill, a useful parameter for identifying the subsequent wind flow, the internal *Froude number,* is defined by:

$$Fr = V/N\delta.$$

Fr represents the ratio of inertial to buoyant forces; high stability implies low Fr although high stability in combination with high V can result in $Fr \approx 1$. Thus, various combinations of stability and wind profile can combine to produce a single Fr value. **Fig. 1.17** shows the variety of flows possible for different stabilities (Fr numbers) for the case of an isolated hill.

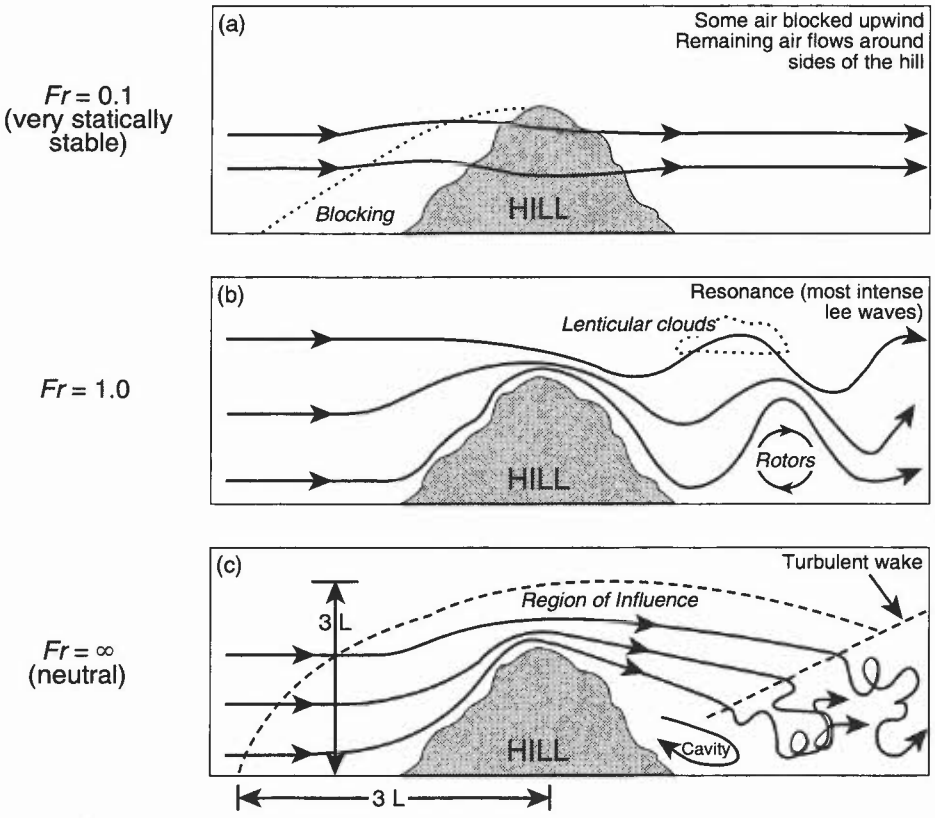

Figure 1.17. Idealized flow over an isolated hill. The Froude number (Fr) compares the natural wavelength of the air to the width of the hill (L). (a) $Fr = 0.1$ (very statically stable), (b) $Fr = 1.0$, and (c) $Fr = \infty$ (neutral).

Summary of guidance on forecasting.

(i) Two types of lee waves can form with different characteristics:
(a) *Trapped waves* form when wind speeds increase with height and/or a less stable layer overlies a stable layer (wave energy is trapped and propagates downwind, confined to low levels).
(b) *Untrapped waves* form if stability is high and/or wind speed low, or the hill width large. The wave energy is propagated upwards so that these waves are routinely observed in the stratosphere, having a characteristic orographic cirrus signature with a well defined boundary (**Fig. 6.1**).

(ii) The length scale of the hills is important — there will be a favoured width of hills depending on the wind and stability conditions.

(iii) An idea of the flow strength may be gained from the distance apart of wave elements on a satellite image. (Flight along the wave, i.e. against and across the flow, can result in experiencing prolonged ascent or descent.)

(iv) Beware of strong-wind situations over the hill top and to its lee where there is an inversion or stable layer not far above the hill or ridge top — this is most likely around the periphery of an anticyclone or ahead of an approaching warm front. Winds can be stronger than expected and quite gusty over the hill top and to its lee. Marked turbulence can be encountered, with perhaps a rotor where the wave flow leaves the ground downwind of the hill.

(v) Both wave types are accompanied by pronounced lee troughing in the surface isobaric field.

(vi) Even in the absence of a stable layer, there will tend to be a flow speed-up effect which may cause the winds over a hill or ridge crest to be as much as double or more the upwind values on occasion, depending on hill height and width.

Both these wave types can generate *severe downslope winds* as as discussed in 1.3.3.4.

Bader et al. (1995)
Barry (1981)
Bradbury (1989)
Bradbury et al. (1994)
Corby (1954)
Foldvick (1962)
Hunt (1980)
Scorer (1949)
Shutts & Broad. (1993)
Starr & Browning (1972)
WMO (1973)

1.3.2.2 Casswell's method for predicting mountain wave characteristics

(i) Casswell presents a graphical method for estimating the likely occurrence and properties of mountain (lee) waves. (This method has little credibility with specialists in the subject.)

(ii) The method involves estimating a parameter l, which is a function of the static stability, the wind speed and vertical wind shear.

(iii) l is allocated a value for two layers (1000–700 and 700–300 hPa) and the existence or not or lee waves read off from a graph. Vertical velocity is then found from a knowledge of the mountain height and wind flow at that height.

Procedure:

(i) From a representative sounding, obtain temperature differences $T_{1000} - T_{700}$ and $T_{700} - T_{300}$.

(ii) From upper-air data obtain:
V_o, the wind at the top of the mountain barrier (surface gradient wind is usually adequate);
V_{850} (or, preferably, mean wind between mountain top and 700 hPa);
V_{500} (or, preferably, the mean 700–300 hPa wind).

(iii) Marked lee waves are not expected if $V_o < 20$ kn or if the direction of V_o makes an angle of $>30°$ with the perpendicular to the mountain range. If lee waves are deemed possible then:
obtain l_{850} from **Fig. 1.18(a)** and l_{500} from **Fig. 1.18(b)**.

(iv) Using l_{850} and l_{500} enter **Fig. 1.18(c)** to obtain L_1, the wavelength (km) and h_1, the height of the maximum vertical velocity, and C_1 (which when multiplied by V_o, gives the maximum vertical velocity). In the figures the ridge height is taken as 300 m. For other values of H multiply the resulting maximum velocity by $H/300$.

(v) Note that $C_1 \times V_o$ m s^{-1} gives vertical velocity in m s^{-1}.

(vi) If the point (l_{850}, l_{500}) lies above tropopause line, no lee waves are expected. If h_1 is above or near the tropopause, any values derived graphically may be unreliable, but marked lee waves are not expected at lower levels.

(vii) If there is a marked decrease of wind speed or change of wind direction at any level, wave activity is not expected to extend beyond this height.

(viii) In a similar way **Fig. 1.18(d)** may be used to determine the likely existence and properties of any secondary wave train at another level above the primary.

(ix) Erroneous results are likely when there is a marked inversion within the wave region. (The maximum vertical velocity should then occur at the base of the stable layer.)

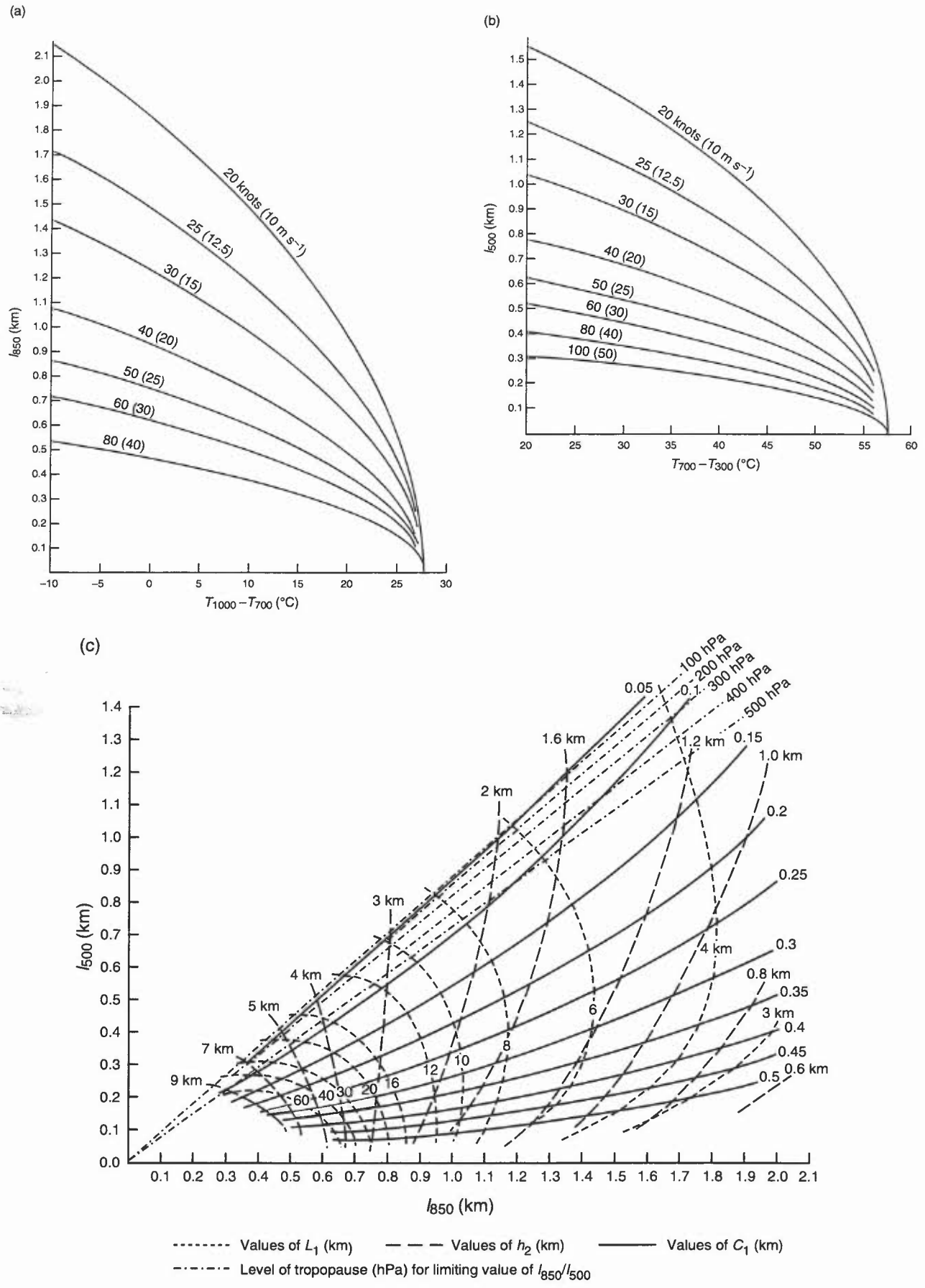

Figure 1.18. (a) Graphs for obtaining (a) l_{850} from $(T_{1000} - T_{700})$ and V_{850}, (b) l_{500} from $(T_{700} - T_{300})$ and V_{500}, (c) L_1, h_1 and C_1, and (d) L_2, h_2 and C_2.

(d)

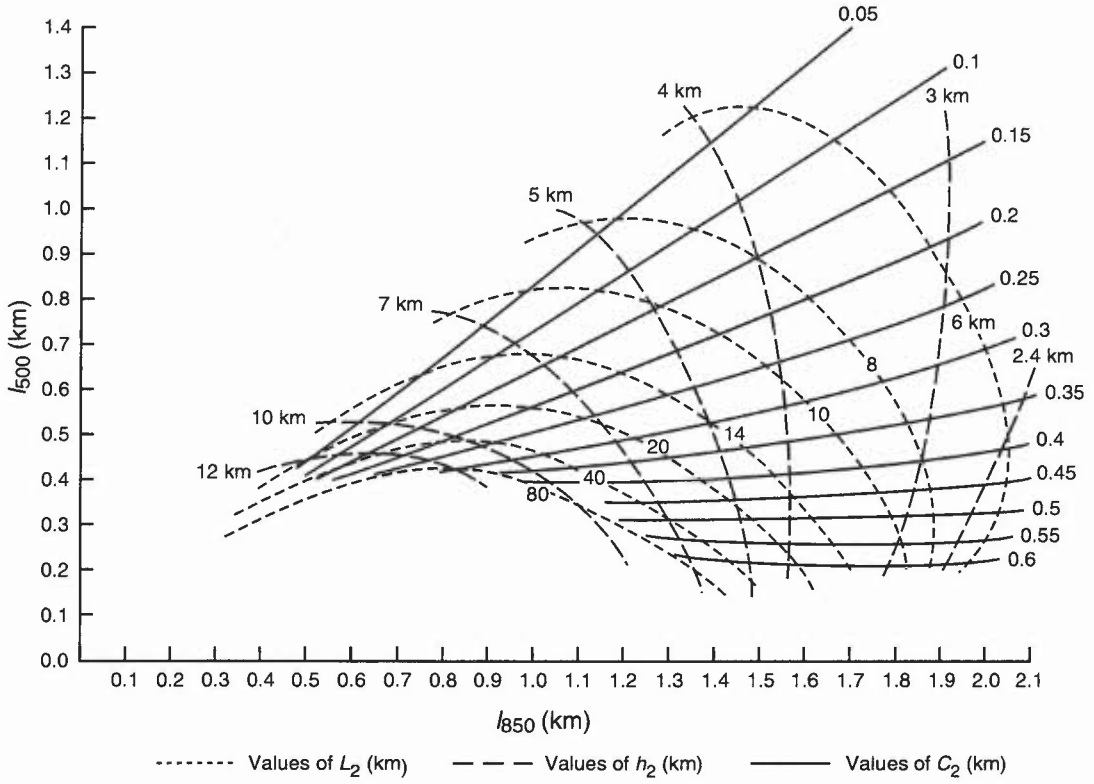

Figure 1.18. (Continued).

Lee waves are generally found when winds are fairly unidirectional, increase in strength with height and when the lowest 3 km has a higher static stability than normal, however, there are numerous cases reported which do not conform to these or other (e.g. HWF) simplified conditions but which are handled well by Shutts' method.

Casswell (1966)

1.3.2.3 Shutts' method for predicting mountain wave characteristics

(i) Shutts' model looks for trapped lee wave modes in a range of directions centred on the near-surface wind direction; it is available as a PC model.

(ii) In the simplified example in **Fig. 1.19** a wind profile that is linear with height is assumed (governed only by values specified at the surface and at a fixed tropopause height of 10 km). The temperature profile is fixed by three values at the surface (12 °C), at 3.5 km (−3 °C) and at the tropopause (−60 °C), the stratosphere being isothermal at that temperature.

(iii) **Fig. 1.19** shows (a) the resonant wavelength, and (b) the maximum vertical velocity and height for a range of surface and tropopause wind speeds. The figure confirms the tendency of the resonant wavelength to increase with wind speed; beyond a certain surface wind they are non-existent. At low wind speeds plots are complicated by the presence of multiple solutions. Between mode regimes, there appear to be regions with no trapped modes. Strong lower tropospheric stability leads to gigantic waves for strong height-independent flows.

The Sheffield storm of 1962 is an example when a lee wave system developed contrary to conventional wisdom, possibly due to trapping of lee waves by reflection off the tropopause (rather than by increasing wind speed with height). The condition for this is that the height of the tropopause should be about $\pi V/N$. This case is handled by Shutts' method.

Aanensen (1965)
Shutts (1992)
Shutts & Broad (1993)

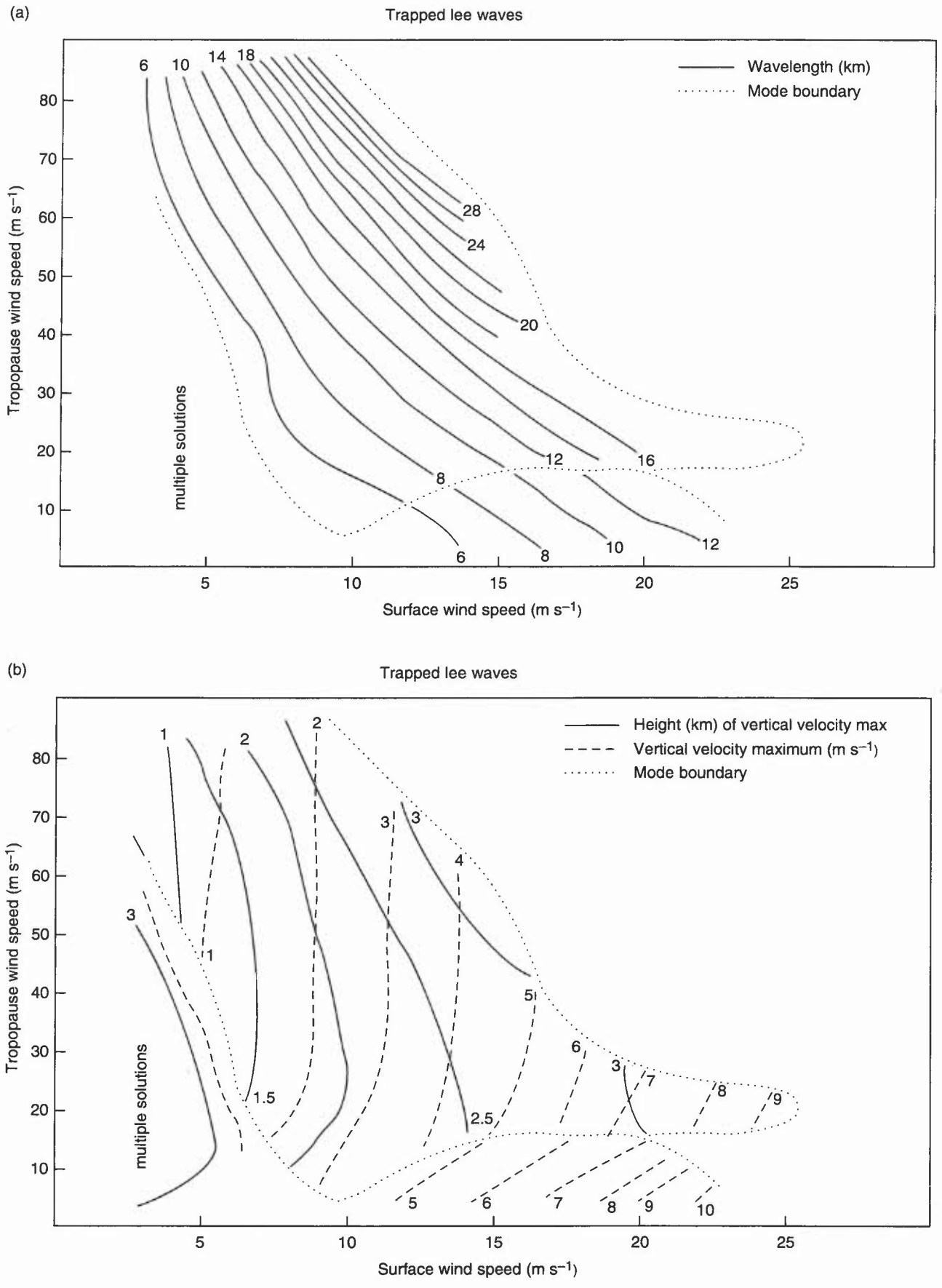

Figure 1.19. (a) Resonant wavelength, and (b) maximum vertical velocity for a range of surface and tropopause wind speeds.

1.3.2.4 *Convection and cloud street waves*

Thermals can act as temporary hills and set off gravity waves in a stable layer, propagating to an altitude of >9 km. (In turn the thermal activity may be stimulated in regions beneath ascending flow and suppressed where wave flow is descending.) This type of wave activity (cloud street waves) requires special criteria:

(i) thermal or cumulus streets lying along the line of the low-level flow;
(ii) the thermal/cloud tops inhibited by an inversion;
(iii) the flow at and above the inversion must blow across the thermal/cumulus streets.

Favourable synoptic conditions are:

(i) weak flow in the convective layer and a horizontal 850 hPa temperature gradient;
(ii) isotherms approximately at right angles to the surface isobars;
(iii) additionally the natural wavelength of the air above the cloud should be similar to the cloud-street spacing.

Booth (1980)
Bradbury (1990)

1.3.2.5 *Speed-up at the crest of an isolated hill*

(i) The fractional speed-up ratio, valid for small slopes (<20°), neutral stability and low hills, is defined as: $\Delta V_{hill} = [V_o(\Delta z)V_A(\Delta z)]/V_A(\Delta z)$
where Δz is the height above the local terrain, subscript 'A' denotes a point upwind where flow is undisturbed and subscript 'o' the hill top.
(ii) For gentle ridges: ΔV_{hill} equals about: 4 × hill height/L
For isolated hills: ΔV_{hill} equals about: 3.2 × hill height/L,
where L is the hill width at half the maximum height of the hill.
(iii) For a typical, gentle hill (height = 100 m, L = 250 m), the speed-up just above the crest can be 160% or more (especially if there is an inversion above summit height).

Stull (1988)

1.3.2.6 *Vertical velocities and slope*

Amplitude of the vertical velocities is determined by the slope of the topography and the undisturbed wind flow, V_A.

Roughly the same characteristics apply for unstable, neutral and slightly unstable lapse rates:

(i) magnitude of vertical velocity is roughly $V_A\tan\alpha$, (where α is ground slope), limited to V_A for $\alpha>45°$;
(ii) slopes <1 in 5 (α about 10°), flow attached to topography;
(iii) slopes 1 in 5 to 1 in 3, flow separation with recirculating eddies downwind; in moist conditions a banner cloud trails away downwind (e.g. Tenerife).
(iv) slopes >1 in 3 ($\alpha \approx 18°$), recirculating eddies down- and up-wind.

An associated characteristic pressure-change signature (a 'kick') of 0.5 to 1 hPa across the hill/ridge may be evident.

Stull (1988)

1.3.2.7 *Airflow over a series of hills*

A series of hills can modify the flow to yield a new profile that behaves in accordance with the characteristics of the rougher surface of the terrain.

Stull (1988)

1.3.2.8 *Airflow with a capping inversion*

An airflow approaching a ridge capped by an inversion will produce **(Fig. 1.20)**:

(i) for relatively slow winds:
acceleration over the ridge crest can locally draw down the inversion;
to the lee of the ridge light winds are found perhaps with flow reversal at low levels;
(ii) for faster winds with a strong capping inversion:
a shallow high velocity lee-slope flow develops, associated with an 'hydraulic jump'.
(iii) if the boundary layer depth is much greater than the hill height:
a flow which tends to evolve as if the hill were not present;

with a shallow boundary layer the air is constrained to flow around the hill, which can give rise to downwind streets of vortices (visible in satellite imagery).

These various responses will be amplified by hill/ridge assymetry.

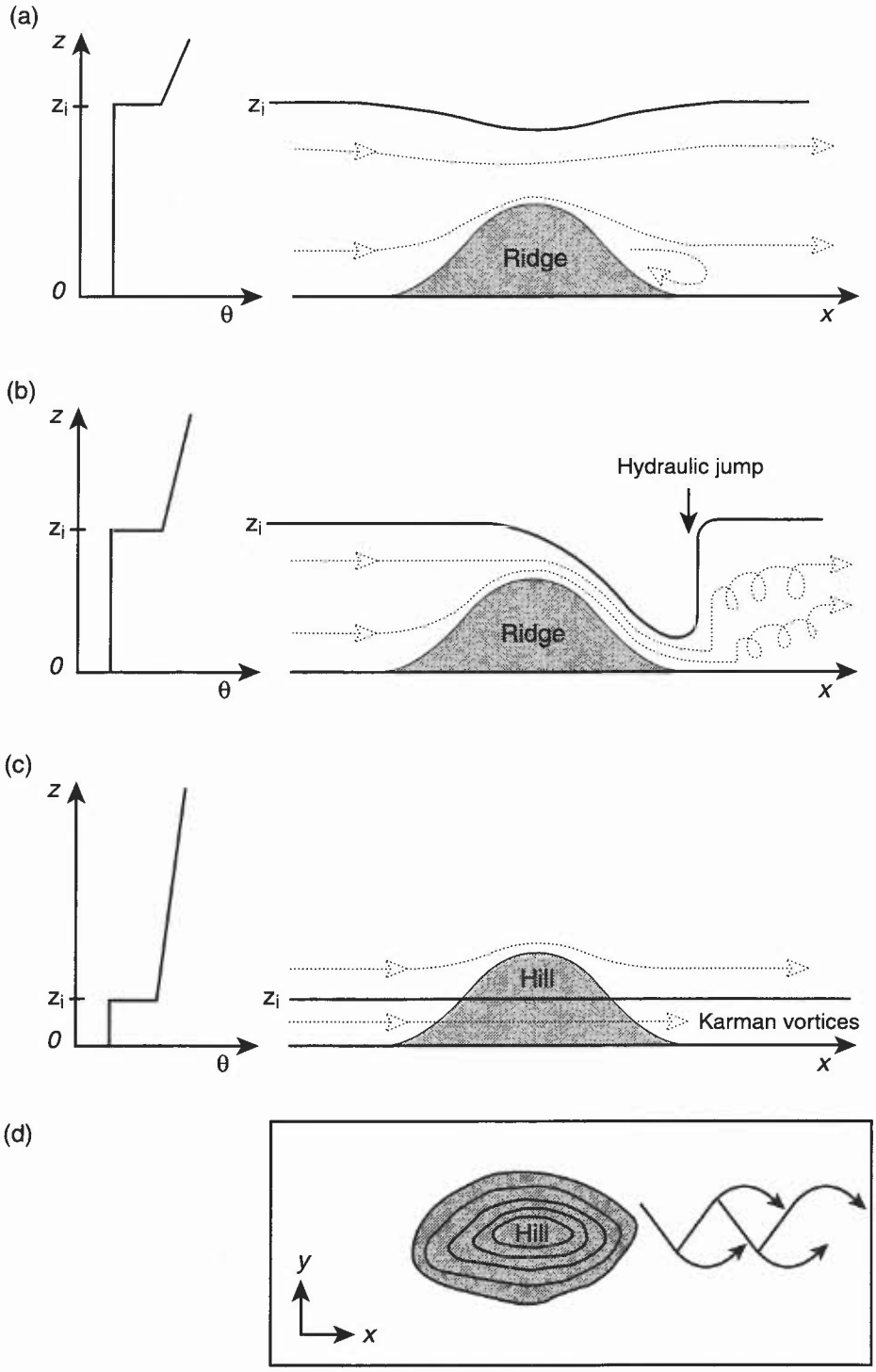

Figure 1.20. (a) Bernoulli effect as flow accelerates over a 2-D ridge, (b) hydraulic jump downwind of a 2-D ridge for greater ambient wind speed, (c) flow around the sides of an isolated hill, and (d) Karman vortex street downwind of the hill from (c). (After Hunt (1980)).

1.3.2.9 Airflow over other complex terrain

(i) Valleys and passes channel wind flows.
(ii) Cross-valley flows can generate both along-valley flow and cross-valley circulations.
(iii) Tall buildings in large cities act like steep valley walls, trapping and channelling air into 'urban canyons'.

1.3.2.10 Airflow over different surfaces

Low-level air flowing from a smooth to a rough surface results in convergence and upward motion above the rough/smooth boundary (the converse holds for rough to smooth flow).

Stull (1988)

1.3.3 Slope and valley winds

1.3.3.1 Anabatic winds:

(i) are generally shallow flows up slopes warmed by solar heating;
(ii) maximum speeds occur within a few metres of the slope surface.

In the United Kingdom these winds are less frequently observed than katabatic winds.

1.3.3.2 Katabatic winds:

These are generally shallow flows (<30 m deep) down slopes and along valleys (donor sites) cooled by nocturnal radiation.

(i) Screen-height fluctuations of temperature and relative humidity have been measured, with a period of about 1 hour, in antiphase.
(ii) An organized wind-shear, perhaps hazardous to aircraft, could be encountered at the bottom as well as at the top of a katabatic airstream, even though the anemometer has ceased to record katabatic flow.
(iii) Another mechanism operates when upper hill slopes are cooled by precipitation, by day or night; the temperature contrast between this cooled air and air at the same level above the lower slopes often results in vigorous katabatic flow.
(iv) A persistent flow results when ground adjacent to sea is snow-covered, resulting in a seaward thermal flow for most of the day.

Bader et al. (1995)
Dawe (1982)
Moffitt (1956)

1.3.3.3 Valley wind systems

On any occasion there may be anabatic or katabatic components complicated by the presence of a gradient wind flow above the level of the surrounding ridge tops and varying through the day as the sun's orientation changes.

Fig. 1.21 illustrates the general pattern, in which there are three main layers with different airflows:

(i) The lowest layer in contact with the slopes flows upwards while the slope is heated and descends towards the valley floor when radiation cools the slopes.
(ii) An intermediate layer where the flow is often reversed. This has been termed the 'anti-wind' which tends to balance the lowest-level flow.
(iii) At the top is the gradient wind, controlled by large-scale synoptic systems.

Bradbury (1989)

1.3.3.4 Severe downslope winds

Two types of mountain waves can generate severe downslope winds (1.3.2.1):

Untrapped lee waves may result in gusty, downslope winds. Conducive atmospheric conditions of high stability accompanying strong low-level flow with little increase in speed with height are frequently found in the lee of the Pennines during:

(i) strong anticyclonic south-westerlies;
(ii) warm-sector conditions;
(iii) in the low-level zone of strong winds a few hundred kilometres ahead of a cold front.

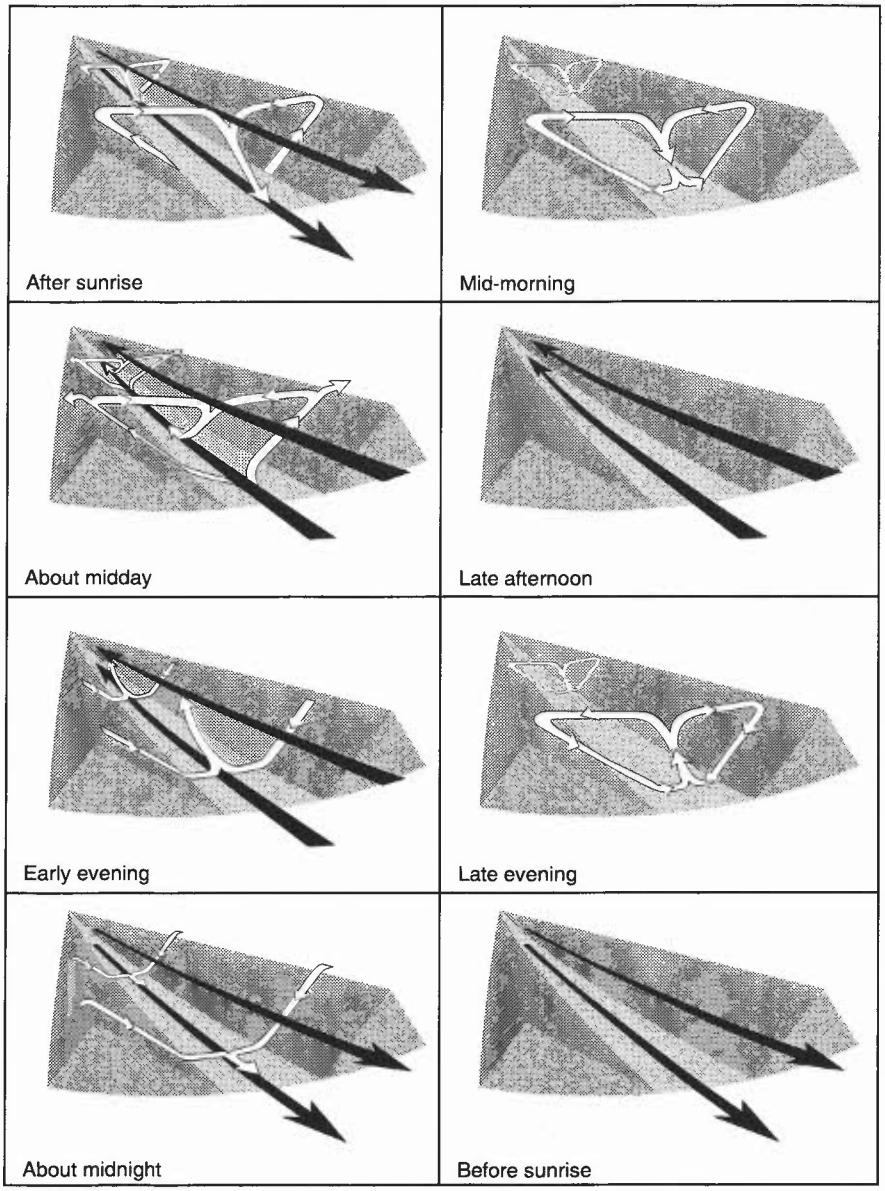

Figure 1.21. Valley wind systems. A schematic display of the diurnal variation of upslope and downslope winds forced by the changing effects of solar heating at the surface.

They are characterized in satellite imagery (e.g. of a frontal system lying across mountainous regions) by dense orographic cirrus in the lee of the mountains; the imagery may show a cloudless 'slot' where frontal cirrus is forced to descend in the lee wave system.

Trapped lee waves may give rise to severe downslope winds when the waves reach a critical amplitude and wavelength.

(i) When the Froude number, based on mountain height (1.3.2.1), is close to unity large amplitude trapped lee waves can form leading to severe downslope winds. UK mountain ridges are never much more than 1 km high so such winds can only occur for $V \approx 10$ m s^{-1}

(ii) The streamlines of flow are concentrated above and to the lee of large mountain ridges (particularly those with steep lee escarpment, such as the western side of the Cross Fell range in the Pennines).

(iii) These extreme winds may extend for some distance across the plain before the flow separates from the surface in an intense vertical current beyond which rotors may be found. Such flow type is analogous to the hydraulic theory of a single fluid layer of constant density as it flows over an obstacle such as a weir and rises again some distance downstream accompanied by turbulent motion.

(iv) Surface charts may show a marked lee trough (note that mesoscale model resolution limitations may result in the effect being underestimated).

Conditions conducive to severe downslope winds resulting from trapped lee waves:
(i) strong stable layer near hill-top height;
(ii) very light winds or flow reversal at some tropospheric level;
(iii) a mountain range with steep leeward escarpment.

The rotor may or may not be indicated by a long roll of ragged cumulus or stratocumulus parallel to the ridge; the 'Helm Bar' in Cumbria is a well-known example.

Both wind regimes require hilly regions of at least 30 km horizontal extent; typical lee-wave related downslope winds in the UK will be associated with a pressure 'kick' across a range of a few hectopascals.

Bader et al. (1995), Chapter 8
Bradbury (1989)
Corby (1954)
Förchtgott (1949)
HAM (1994)
Klemp (1978)
Stull (1988)

1.3.3.5 Rotor streaming (see 6.2)

1.3.3.6 Föhn winds

(i) Föhn winds occur on the lee side of mountain ranges when the winds aloft blow across the axis of the main ridges. Two examples are shown in **Fig. 1.22.**
(ii) In the more common 'subsidence' case **(a)**, low-level cold air flow is blocked upstream and only the higher-level flow crosses the ridge to plunge down the lee side as a very dry, adiabatically warmed, current.
(iii) In **(b)** all the upstream air crosses the ridge. Orographic lifting produces cloud; precipitation over the mountains then depletes the moisture content; the drier air then descends the lee side, warming adiabatically.

Bader et al. (1995), Chapter 8
Bradbury (1989)
Lawrence (1953)

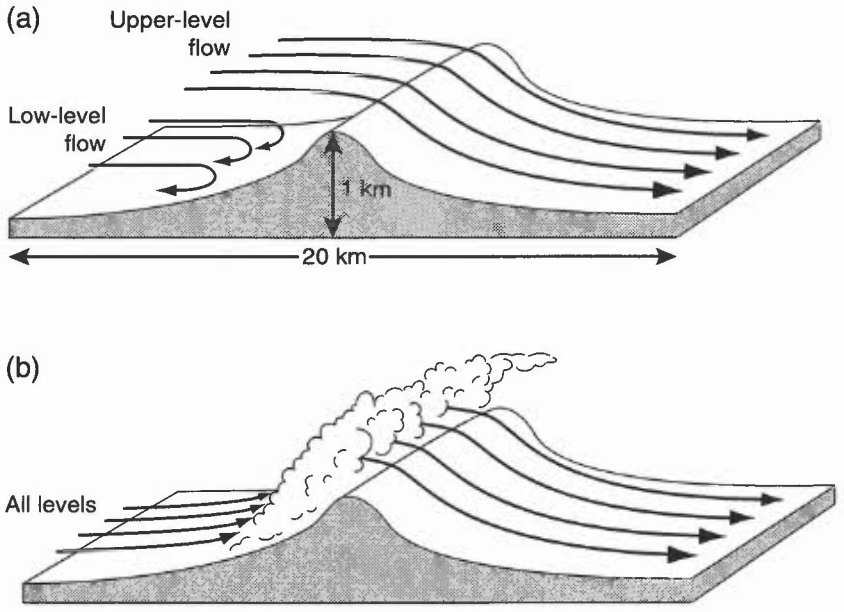

Figure 1.22. Föhn winds. (a) The low-level flow is blocked upstream of the hill barrier and only the higher-level air flows across the ridge, and (b) all the upstream air crosses the ridge.

1.3.4 Urban winds

Gusts and lulls due to channelling by buildings and streets result in eddies around the sides and in the precincts in front of (tall) structures, strengthening winds by up to a factor of three. Restricted and channelled air movement under appropriate synoptic conditions can result in high levels of air pollutants at ground level in the so-called 'canopy layer'.

The temperature differential due to the urban 'heat island' (2.11) can set up a 'country breeze', a low-level flow (<8 kn) of cool air from the rural area towards the city. Contrarotating eddies have been measured over opposite sides of a city. Frictional drag over large cities reduces wind speeds below that of the rural surroundings; pollution can be transported large distances downwind in the 'urban plume' which is as wide as the city, and whose boundary-layer characteristics vary diurnally **(Fig. 1.23)**.

Oke (1982)
Stull (1988)

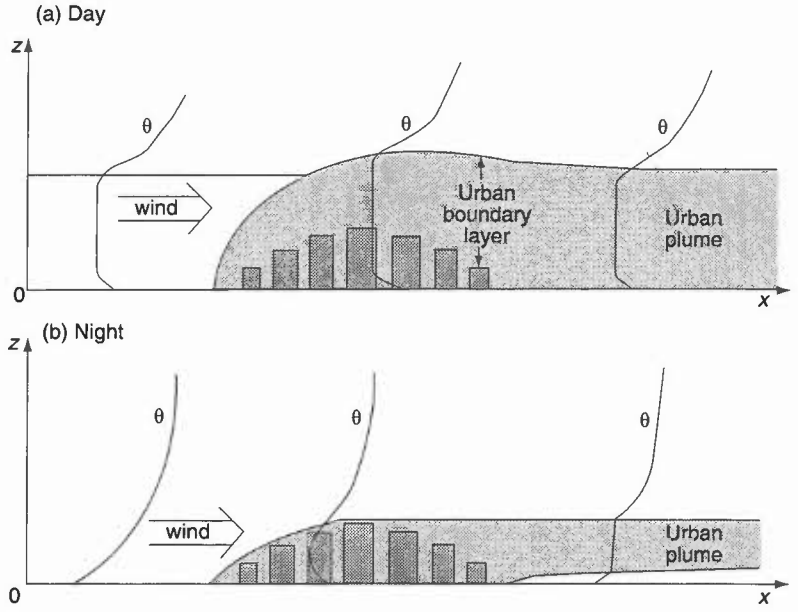

Figure 1.23. Sketch of urban boundary layer and urban plume for (a) a windy day and (b) a windy night (after Oke (1982)).

1.3.5 Wind-chill (see 2.10)

BIBLIOGRAPHY

CHAPTER 1 — WIND

Aanenson, C.J.M. (Editor), 1965: Gales in Yorkshire in February 1962. *Geophys Mem* No. 108, Meteorological Office

Bader, M.J., Forbes, G.S., Grant, J.R., Lilley, R.B.E. and Waters, J., 1995: Images in weather forecasting. Cambridge University Press.

Barry, R.G., 1981: Mountain weather and climate, Methuen.

Booth, B., 1980: Unusual wave flow over the Midlands. *Meteorol Mag*, **109**, 313–324.

Bradbury, T.A.M., 1989: Meteorology and flight, A & C Black.

Bradbury, T.A.M., 1990: Links between convection and waves. *Meteorol Mag*, **119**, 112–120.

Bradbury, W.M.S., Deaves, D.M., Hunt, J.C.R., Kershaw, R., Nakamura, K. and Hardman, M.E., 1994: The importance of convective gusts. *Meteorol Appl*, **1**, 365–378.

Brittain, O.W., 1970: Forecasting the inland penetration of a sea-breeze over Lincolnshire. Met. Office Forecasting Techniques Memorandum No. 20.

Carruthers, D.J. and Choularton, T.W., 1982: Airflow over hills of moderate slope. *QJR Meteorol Soc*, **108**, 603–624.

Casswell, S.A., 1966: A simplified calculation of maximum vertical velocities in mountain lee waves. *Meteorol Mag*, **95**, 68–80.

Corby, G.A., 1954: The airflow over mountains: A review of the state of current knowledge. *QJR Meteorol Soc*, **80**, 377–408.

Dawe. A.J., 1982: A study of a katabatic wind at Brueggen on 27 February 1975. *Meteorol Mag*, **111**, 491–521.

Findlater, J., 1964: The sea breeze and inland convection — an example of the interrelation. *Meteorol Mag*, **93**, 82–89.

Findlater, J., Harrower, T.N.S., Howkins, G.A. and Wright, H.L., 1966: Surface and 900 mb wind relationships. Scientific Paper No. 23. London, HMSO.

Foldvick, A., 1962: Two-dimensional mountain waves — a method for rapid computation of lee wavelength and vertical velocity. *QJR Meteorol Soc*, **88**, 271–285.

Förchtgott, J., 1949: Wave currents on the leeward side of mountain crests. *Bull met tchecoal, Prague*, **3,** 49–51.

HAM. Handbook of Aviation Meteorology, 1994: London, HMSO.

HWF. Handbook of Weather Forecasting, 1975: Met.O.875, Meteorological Office.

Holton, J.R., 1992: Introduction to dynamic meteorology (3rd edition). Academic Press.

Hunt, J.C.R., 1980: Wind over hills. Workshop on the Planetary Boundary Layer, pp. 107–144. Am Meteorol Soc.

Hunt, J.C.R., 1995: The contribution of meteorological science to wind hazard mitigation. *In* T. Wyatt (Ed), Proceedings of the Wind Engineering Society meeting on wind hazard, May 1995.

Klemp, J.B., 1978: A severe downslope windstorm and aircraft event induced by a mountain wave. *J Atmos Sci*, **35**, 59–77.

Lawrence, E.N., 1953: Föhn temperatures in Scotland. *Meteorol Mag*, **82**, 74–79.

Ludlam, F.H., 1980, Clouds and storms. Pennsylvania State University Press.

McCarthy, J. and Serafin, R., 1984: The microburst: hazard to aircraft. *Weatherwise*, **37**, 120–127.

Mason, P.J., 1986: Flow over the summit of an isolated hill. *Boundary Layer Meteorol*, **37**, 385–405.

Meteorological Glossary (MG) (6th Edition), 1991: London, HMSO.

Meteorological Office (Heathrow), 198?

Moffitt, B.J., 1956: The nocturnal wind at Thorney Island. *Meteorol Mag*, **85**, 268–271.

Oke, T.R., 1982: The energetic basis of the urban heat island. *QJR Meteorol Soc,* **108**, 1–24.

Pielke, R.A., 1984: Mesoscale meteorological modeling. Academic Press, Florida.

Scorer, R.S., 1949: Theory of waves in the lee of mountains. *QJR Meteorol Soc*, **75**, 41–56.

Shutts, G.J., 1992: Observations and numerical model simulation of a partially trapped lee wave over the Welsh mountains. *Mon Weather Rev*, **120**, 2056–2066.

Shutts, G.J. and Broad, A., 1993: A case study of lee waves over the Lake District in northern England. *QJR Meteorol Soc*, **119**, 377–408.

Simpson, J.E., 1994: Sea breeze and local wind. Cambridge University Press.

Starr, J.R. and Browning, K.A., 1972: Observations of lee waves by high power radar. *QJR Meteorol Soc*, **98**, 73–85.

Stull, R.B., 1988: An introduction to boundary layer meteorology. Kluwer Academic Publishers.

Thorpe, A.J. and Guymer, T.H., 1977: The nocturnal jet. *QJR Meteorol Soc*, **103**, 633–654.

WMO, 1969: Vertical wind shear in the lower layers of the atmosphere. Geneva, World Meteorological Organization, Technical Note 93.

WMO, 1973: Airflow over mountains. Geneva, World Meteorological Organization, Technical Note 127.